Random Waves on a Vertically-sheared Current

C. Swan[1] and R. L. James[2]

Abstract

This paper considers the interaction between two-dimensional random waves and a co-linear, depth-varying, current. Two rotational wave-current models, capable of incorporating the effects of a depth dependent vorticity distribution, are combined with a conservation equation describing the total energy flux. This provides new solutions capable of predicting the change in a wave spectrum due to the interaction with a current. Comparisons between these solutions and a new data set confirms that a successful wave-current model must incorporate both the Döppler shift associated with the surface current and the near-surface vorticity distribution. Typical design calculations, based on a uniform current approximation, commonly satisfy neither of these constraints. Accordingly, they are shown to provide a poor description of the laboratory data. Furthermore, the nature of the wave-current interaction, which is shown to be significantly larger than the nonlinear wave-wave interactions, involves both a current-induced change in the wave motion and a wave-induced change in the current. While the former is reasonably well understood, the latter remains difficult to predict. Indeed, both parts of this overall interaction are shown to be strongly vorticity dependent.

1. Introduction

The nonlinear interaction between waves and a co-existing current is an important feature of many coastal and offshore environments. Accordingly, several authors have considered the case of regular waves on a variety of current profiles (see, for example, the recent review article by Thomas and Klopman, 1997). In its simplest form the current profile, $U(z)$, is assumed to be uniform with depth. In this case no vorticity is present and it has been conclusively shown that both the dispersion equation and the associated water particle kinematics are well described by a Döppler shifted solution (Fenton, 1985). Likewise, the change in the wave height, ΔH, which arises when the waves first propagate onto the current, can be modelled via the conservation of wave action

[1] Reader and [2] Research Assistant, Department of Civil and Environmental Engineering, Imperial College, London SW7 2BU.

(Thomas, 1990). Alternatively, if it is assumed that the current profile is represented by a linear shear, then a uniform vorticity distribution (ω=dU/dz) is introduced. In this case the wave motion again remains irrotational, but additional vorticity dependent terms arise within the dispersion equation so that the Döppler shifted solution is no longer applicable. In this case the water particle kinematics have been considered by Tsao (1959) and Kishida and Sobey (1988); while a linear formulation of a conservation equation for wave action has been provided by Jonsson *et al.* (1988).

More recently, solutions have been presented which address the case of waves on a current profile that varies arbitrarily with depth. In particular, considerable attention has been paid to cases in which the current profile is strongly sheared close to the water surface. Such cases are practically important since they are representative of a wind-driven current, and may also correspond to a typical estuarine outfall in the near-shore coastal region. In these cases the vorticity distribution is strongly non-uniform and, consequently, the wave motion becomes rotational. In terms of kinematic predictions an analytical model describing this type of interaction has been proposed by Swan (1992) and recently modified by Swan and James (1998); while numerical formulations are provided by Dalrymple (1974), Chaplin (1990), Thomas (1990) and Cummins and Swan (1993). In contrast, the initial wave height change, ΔH, caused by the interaction with a strongly sheared current is more difficult. In the absence of an appropriate (nonlinear) conservation of wave action equation, the conservation of total energy flux, R_x, must be applied.

Although the advances noted above have greatly enhanced our understanding of nonlinear wave-current interactions, they are restricted in the sense that they have principally considered the case of regular waves on currents. In practice the waves observed in most offshore and coastal locations are random, or irregular, with a significant frequency spread. In these cases the design engineer may be primarily concerned with the changes in a wave spectrum due to the interaction with a sheared current. It is this task which the present paper will address. Section 2 commences with a description of the experimental facility in which two-dimensional random waves were super-imposed on a depth-varying current. The essential characteristics of both an analytical wave-current model (Swan and James, 1998) and a multi-layered numerical model (Cummins and Swan, 1993) are briefly outlined in section 3. Using these results, a conservation of total energy flux equation is outlined, and verified with comparisons to a fifth-order conservation of wave action equation (Thomas, 1990) for the simplified case of regular waves on a uniform current. Comparisons between the laboratory data and both the analytical and numerical models are presented in section 4; while section 5 provides some concluding remarks concerning the extent of the wave-current interaction, the importance of the vorticity distribution, and those areas which require further consideration.

2. Experimental Apparatus and Measuring Procedure

The experimental work undertaken within this study was conducted in a purpose built wave-current flume. This facility is located in the Hydraulics Laboratory within the

Department of Civil and Environmental Engineering at Imperial College, London. The flume has an overall length of 25m, a width of 0.3m, and a working depth of 0.7m. The waves are generated by a bottom-hinged, numerically controlled, wave paddle located at one end of the wave flume. At the opposite end the wave energy is absorbed by a large block of poly-ether foam, the front face of which is cut to form a vertical wedge with an included angle of 30°. With this passive absorber in place, the reflection coefficient across a broad range of regular wave conditions was less than 2%. Further details of the wave flume are provided by Baldock *et al.* (1996).

Within the present tests the current was introduced via three loops of pipework. These allow a re-circulating and reversible current with a maximum volume discharge of $0.05m^3/s$. A sketch indicating the layout of the experimental facility is given on figure 1. Measurements undertaken within the wave-current flume include both time-histories of the water surface elevation, $\eta(t)$, recorded at a number of fixed spatial locations, and point measurements of the water particle kinematics to define both the shape of the current profile (acting in the absence of the waves) and the extent of the wave-current interaction. The surface elevation data was recorded via an array of surface-piercing resistance gauges. Individually, these consist of two vertical wires, each with an external diameter of 1mm, placed 10mm apart. Previous experience has shown that these gauges cause almost no disturbance of the flow field, and allow the water surface elevation to be recorded with an accuracy of ±1mm. The velocity data was recorded using a three beam Laser Döppler anemometer based on a 30mW helium-neon laser. This system was established in a forward scatter mode for optimal signal to noise ratio, and allows two components of the water particle velocity to be recorded simultaneously with an accuracy of ±2%. In each of the cases presented the measuring section was located 2.8m downstream of the wave paddle.

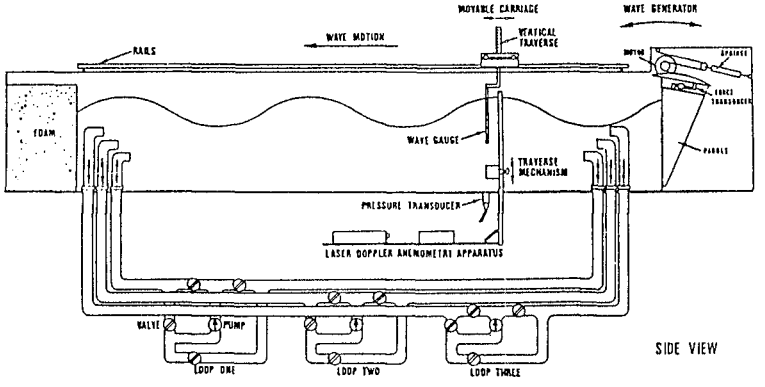

Figure 1. Layout of experimental facility

To create a vertically-sheared current at the measuring section, the mean flow was introduced in the form of an upwelling immediately downstream of the wave paddle (figure 1). With careful modifications of the inlet conditions a steady, two-dimensional,

current was achieved in which the surface velocities were of the order of $U_{z=\eta}\approx 0.6$m/s and the surfaee vorticity was as large as $(dU/dz)_{z=\eta}\approx 2.0$m/s/m. Figure 2a describes the time-variation of the current profile over a period of 3 hours; while figure 2b describes the cross-tank variation. These results clearly suggest that the eurrent profile is both steady and two-dimensional. In contrast, figure 2c describes the downstream variation in the current profile. Although there clearly remains some downstream variation, i.e. $dU/dx\neq 0$, this is at least one order of magnitude smaller than the gradient in the z direction. Hence, we are able to conclude that the nature of the wave-current interaction is dominated by the vertical shear in the current profile.

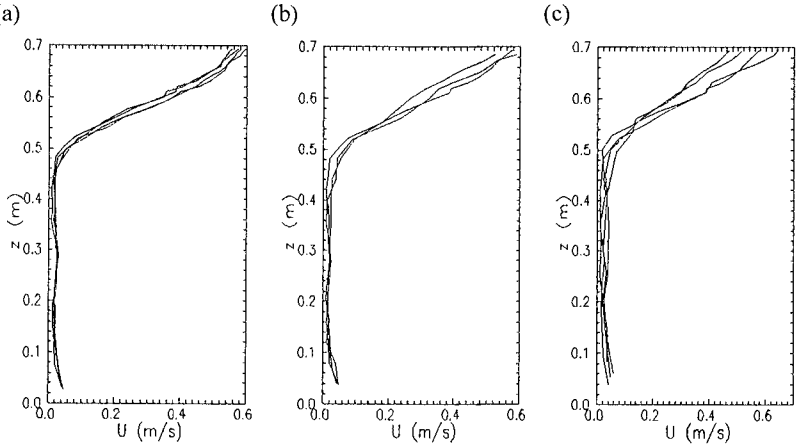

Figures 2a-2c. Characteristics of the current profile.
(a) Variation with time: t=0, 1hr, 2hrs and 3hrs; (b) Cross-tank variation: y=0.25b, 0.5b and 0.75b; (c) Downstream variation: x=0, 1.4m, 2.1m and 2.8m.

3. Modelling Work

In this section we will briefly mention two methods which have previously been applied to the modelling of regular waves on depth-varying currents. The first is the multi-layered numerical model outlined by Cummins and Swan (1993); while the second corresponds to the weakly nonlinear analytical solution described by Swan and James (1998). Although the results of these models are shown to be in good mutual agreement, the latter model is much easier to apply in the context of random waves. Indeed, the agreement between these models is an important finding in itself since it implies that the analytical formulation, which is only accurate to a second-order of wave steepness, has a wider range of applicability than one might expect.

3.1 Numerical Modelling

The scheme proposed by Cummins and Swan (1993) is essentially a five-layered equivalent of the two-layered or bi-linear shear model originally proposed by Dalrymple

(1974). If the computational domain is defined according to figure 3a, the stream function, ψ, in the i^{th} fluid layer, where i=1, ..., 5, is given by:

$$\psi = (c - U_{(i-1)})z - \frac{(U_i - U_{i-1})}{d_{i-1} - d_i}\left(\frac{z^2}{2} + d_{i-1}z\right) + \sum_{n=1}^{N}\left[X_i(n)\sinh\left(\frac{2\pi nz}{\lambda}\right) + Y_i(n)\cosh\left(\frac{2\pi nz}{\lambda}\right)\right]\cos(nkx) \quad (1)$$

where the Cartesian co-ordinates (x,z) have their origin at the mean water surface, z is measured vertically upwards and x in the direction of wave propagation, c is the phase velocity, d_i is the depth of the i^{th} fluid layer, U_i defines the current profile, and λ is the wave length. Within (1) the first term on the right hand side ensures that the solution is steady; the second term defines the current profile, approximated by a series of linear shear currents; while the third term defines the oscillating flow field and includes the unknown coefficients (X_i, Y_i). A solution of this type is appropriate to the description of the equilibrium conditions arising in a combined wave-current flow.

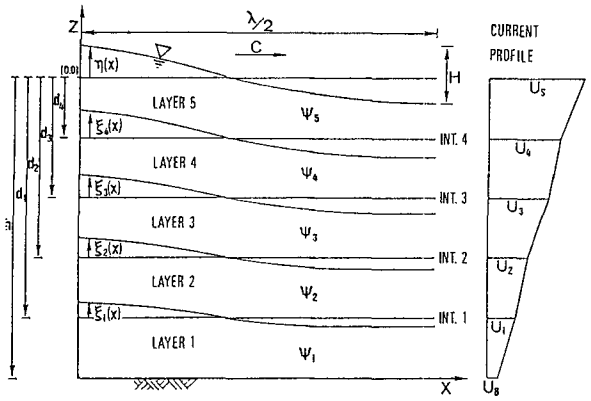

Figure 3a. Co-ordinate arrangement and solution domain

Assuming that the wave height, H, the wave period, T, the water depth, d, and the current profile, $U(z)$ (occurring in the presence of the waves) are defined, the usual boundary conditions coupled with a number of compatibility constraints applied at the interfacial sections ($z=\xi_i$, where i=1, ..., 5) allow the flow field to be solved. Solutions for the wave length, λ, the surface profile, η, the oscillatory velocity components (u,v) and the pressure, p, are thus achieved. Using this approach the order of the approximation was typically set at N=8 for nonlinear waves on a strongly sheared current, and the calculations undertaken on a standard 200MHz personal computer. Detailed comparisons between this model and a data set concerning regular waves on a variety of strongly sheared currents are provided by Swan *et al.* (1998).

3.2 Analytical Modelling

In contrast to the numerical scheme noted above, the analytical model is restricted to a second-order of wave steepness and is based on the orthogonal transformation indicated on figure 3b.

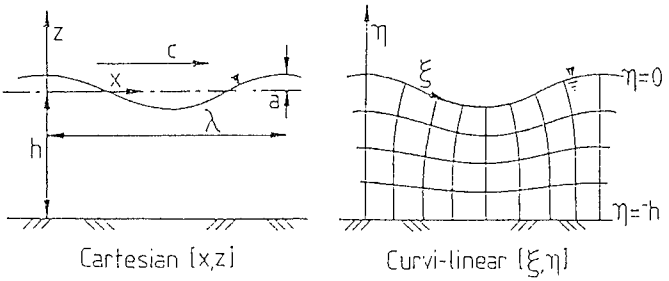

Figure 3b. Co-ordinate arrangement and solution domain

Within the (ξ,η) frame, η=0 defines the free-surface, η=-d, the bottom boundary, and the current profile (again specified in the presence of the waves) is defined by a third-order polynomial such that in a stationary frame of reference:

$$U(\eta) = (P + 2Q\eta + 3R\eta^2 + 4S\eta^3).\delta_s(\eta + md) \tag{2}$$

where P, Q, R and S are constants, η=-md defines the vertical extent of the current, i.e. $0 \le m \le 1$, and δ_s is a step function such that $\delta_s(y)$ is 0 if $y<0$ or 1 if $y \ge 0$. After solving the two-dimensional vorticity equation in general orthogonal co-ordinates for an inviscid fluid, subject to the usual boundary conditions, the stream function, ψ, is given by:

$$\begin{aligned}\psi = &-c\eta + \left(Q\eta^2 + R\eta^3 + S\eta^4\right)\delta_s(\eta + md) - P\eta.\delta_s(-\eta - md)\\ &+ a\left(2Q\eta + 3R\eta^2 + 4S\eta^3 + \frac{6S\eta}{k^2} + f_a\right)\frac{\sinh k(d+\eta)}{\sinh(kd)}\cos(k\xi).\delta_s(\eta + md)\\ &+ a\left(-\frac{3R\eta}{k} - \frac{6S\eta^2}{k} + f_b\right)\frac{\cosh k(d+\eta)}{\sinh(kd)}\cos(k\xi).\ \delta_s(\eta + md)\\ &+ af_c \sinh k(\eta + md)\cos(k\xi).\delta_s(-\eta - md)\end{aligned} \tag{3}$$

where the constant coefficients f_a, f_b and f_c are dependent on the wave characteristics and the current profile. Applying this solution, the velocity components in the (ξ,η) directions are given by:

$$u_\xi = J^{1/2}\frac{\partial\psi}{\partial\eta} \quad \text{and} \quad u_\eta = -J^{1/2}\frac{\partial\psi}{\partial\xi} \tag{4}$$

where the Jacobian, J, is defined by $J=\partial(\xi,\eta)/\partial(x,z)$. Within this solution the first term on

the right side of (3) reflects the translation of the co-ordinate axis; the second and third terms define the current profile; while the remaining terms provide a first approximation to the nonlinear wave-current interaction. Comparisons between this solution, the numerical model discussed in section 3.1, and a number of regular wave cases on strongly sheared currents, are provided in Swan and James (1998). This paper also gives explicit solutions for the Jacobian and the dispersion equation.

3.3 Energy Flux

We have already noted that in the case of nonlinear waves interacting with a strongly sheared current (with non-uniform vorticity) a conservation equation for wave action has not, as yet, been derived. Accordingly, a simpler approach, orginally proposed by Longuet-Higgins and Stewart (1960) in their derivation of the radiation stress tensor, is adopted. This ensures that the total energy flux associated with both the wave and the current is conserved. In effect, the total energy flux comprises three distinct contributions. The first arises due to the rate at which work is done by the pressure, p. If we consider the combined wave-current flow, this contribution is defined by:

$$R_x^1 = \iint p\,u_x\,dz\,dx \tag{5}$$

where u_x is the total horizontal velocity including both the wave and the current components, i.e. $u_x=u+U$. The second contribution arises from the additional transport of kinetic energy and is given by:

$$R_x^2 = \int\int \left(\tfrac{1}{2}\rho\,\underline{u}^2\right) u_x\,dz\,dx \tag{6}$$

where ρ is the density of the fluid and $\underline{u}=u_x+u_z$. Similarly, the third contribution represents an additional transport of potential energy and is given by:

$$R_x^3 = \int\int (\rho\,g\,z)\,u_x\,dz\,dx \tag{7}$$

where g is the gravitational acceleration and d the total water depth. Combining these results gives a total energy flux of $R_x = R_x^1 + R_x^2 + R_x^3$. Assuming that this total flux is constant, one can add the energy flux associated with the current (acting alone) with the energy flux associated with the waves (again acting alone), and equate this to the total energy flux in the combined wave-current environment:

$$R_{x(\text{current})} + R_{x(\text{waves})} = R_{x(\text{waves+current})} \tag{8}$$

If this equation is combined with the results of either the numerical model (section 3.1) or the analytical solution (section 3.2) the wave height change, ΔH, which arises when the wave and the current first interact, can be determined.

To verify this energy flux formulation we first considered a simple waves only situation (no current) and compared the sum of (5), (6) and (7) with the energy flux

calculated according to Ec_g, where E is the energy in one wave length and c_g is the group velocity. Figure 4a presents the results of this comparison for regular waves (T=10s, d=50m) in which Ec_g was calculated using a high-order stream function solution. The observed agreement is clearly very good, with minor deviations only arising in the very steepest waves. In a second test, we considered the case of regular waves (H=7.5m, T=10s, and d=50m) propagating on a uniform current. In this case the wave height change predicted using the present formulation, i.e. (8), coupled with a high-order stream function solution was compared to the linear solution proposed by Bretherton and Garrett (1968) and the fifth-order solution proposed by Thomas (1990). The latter solutions being based upon the conservation of wave action. Figure 4b contrasts these results and shows good agreement between the present energy flux approach and the nonlinear conservation of wave action. Indeed, this figure also highlights the importance of the nonlinear terms when seeking to define the change in wave height.

4. Discussion of Results: Random Waves

The solutions outlined in sections 3.1 and 3.2 were formulated to solve the interaction of regular waves with depth-varying currents. Nonetheless, they can be applied in a 'linear' sense to the individual components of a random or irregular sea in an attempt to determine a first approximation to the changes in the wave spectra. If this approach is adopted, the nonlinear interaction between the individual wave components and the co-existing current are correctly modelled, but the nonlinear wave-wave interactions (together with any subsequent interactions that these components have with the current) are neglected. However, it will be shown that for a typical Pierson-Moskowitz (P-M) spectrum interacting with a strongly sheared current, the nonlinear wave-wave interactions are negligible in comparison to the wave-current interactions. As a result, the present approach should provide a good first approximation to any changes in the wave spectrum.

The first P-M spectrum investigated in the laboratory study had an average zero up-crossing period of T_z=0.94s and a significant wave height (measured in the absence of a current) of H_s=0.062m. This case therefore corresponds to a relatively linear sea state. The characteristics of this spectrum measured on quiescent water (or in the absence of a current) are indicated by the uppermost curve on figure 5a. This spectrum was generated by the summation of 99 individual wave components with random phasing; it was calculated from two time-histories of the water surface elevation, each recorded at 25Hz for a duration of 600s. Preliminary tests confirmed that this spectrum was highly repeatable, being both stationary and ergodic. In subsequent tests the current profile indicated on figure 2a was generated within the wave flume. Having allowed sufficient time for the profile to become stable, an identical signal to that described above was sent to the wave paddle. The resulting water surface elevations, involving the waves on the current, were again recorded and the corresponding spectra calculated in an identical manner. The results of this process are indicated by the second solid line on figure 5a. The effect of the wave-current interaction, in terms of spectral changes, is clearly apparent.

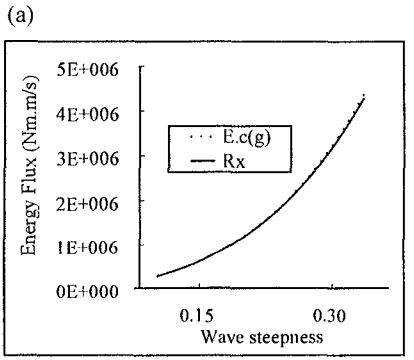

Figure 4a. Energy flux for waves only case

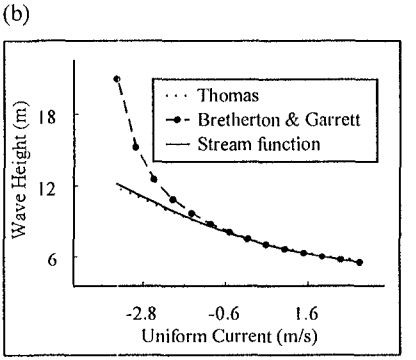

Figure 4b. Wave height change on a uniform current

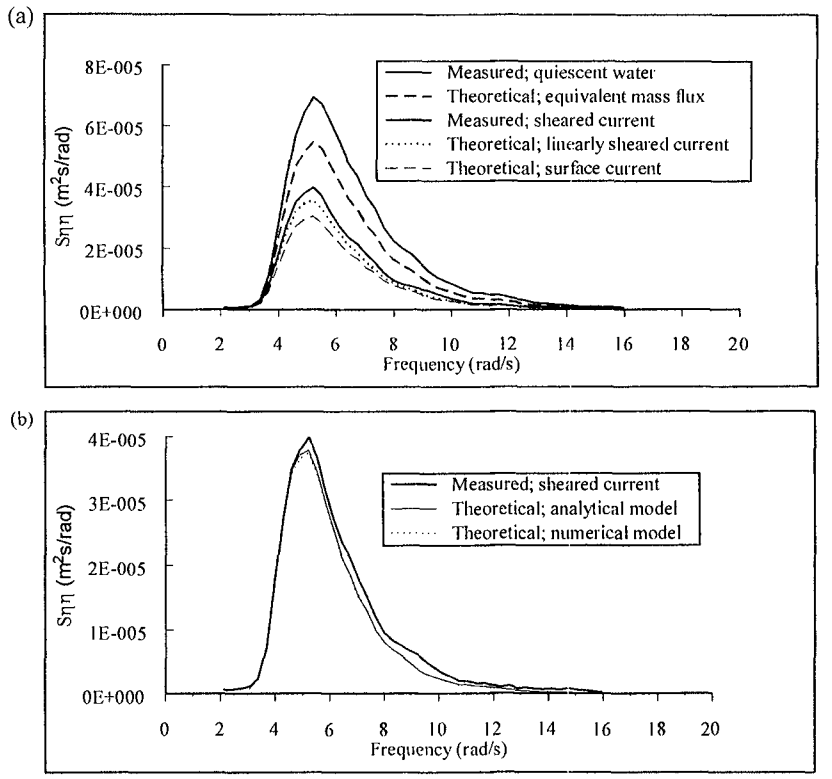

Figure 5a-5b. Changes in a linear spectrum

The remaining curves indicated on figure 5a correspond to the predicted wave spectrum assuming that: (a) the current is uniform with depth and has a value equal to the surface current; (b) the current is uniform with depth and has a value such that the total (depth-integrated) mass flux is conserved; and (c) the current varies linearly with depth. These comparisons suggest that while solution (a) correctly models the Döppler shift, it entirely neglects the vorticity and therefore over-predicts the change in the wave spectrum. Alternatively solution (b), which is commonly applied in a design context, fails to model either the Döppler shift or the vorticity profile, and consequently provides the worst prediction of the wave-spectra on the current. In contrast, the solution which uses a linearly-sheared current correctly describes the Döppler shift, and makes some attempt to model the effects of the vorticity. As a result, this latter model provides an improved description of the measured spectra. Nevertheless, even in this case, there remain significant differences between the measured and predicted data.

In contrast figure 5b compares the wave spectra measured on the current with the results of both the numerical model and the analytical solution described in sections 3.1 and 3.2. In each of these solutions iterative calculations were undertaken to determine the individual wave heights which satisfy the total energy flux constraint (8). In applying this approach it is assumed that there is no transfer of energy between components within the spectrum. This point is further discussed below. Furthermore, it is important to note that although the iterative calculations are relatively straightforward, those based on the numerical model can be somewhat time-consuming. Whereas those based on the analytical model are rapid and easy to apply. In essence, this latter solution is no more difficult to apply than a second-order Stokes' model.

The comparisons provided on figure 5b confirm that both these solutions provide a much improved description of the wave spectra measured in the presence of the current. Indeed, this is to be expected since these models (and only these models) allow the affects of both the Döppler shift and the vorticity distribution to be correctly incorporated. Furthermore, comparisons between figures 5a and 5b suggest that the vorticity can be of equal importance to the Doppler shift when attempting to predict the changes in the wave spectra due to the interaction with a sheared current.

Figures 6a and 6b present a similar sequence of results in which the P-M spectrum measured in quiescent water has an average zero up-crossing period of T_z=0.98s and a significant wave height of H_s=0.090m. In this case the sea-state is more nonlinear, with some evidence of occasional wave breaking. However, the frequency of the breaking events was such that they had no significant influence on the characteristics of the wave spectrum. In figure 6a the measured and predicted spectra show similar trends to those identified on figure 5a, although the differences are inevitably somewhat larger. This is particularly true of the linearly-sheared current (Jonsson *et al.*, 1978) since this neglects the nonlinear terms in the wave-current interaction. Figure 6a also includes an additional curve, which indicates the magnitude of the second-order nonlinear wave-wave interactions (the scale appropriate to this curve is given on the right hand axis). Comparisons between this curve and the change in the wave spectrum due to the interaction with the current confirm that the wave-current interaction is indeed dominant.

(a)

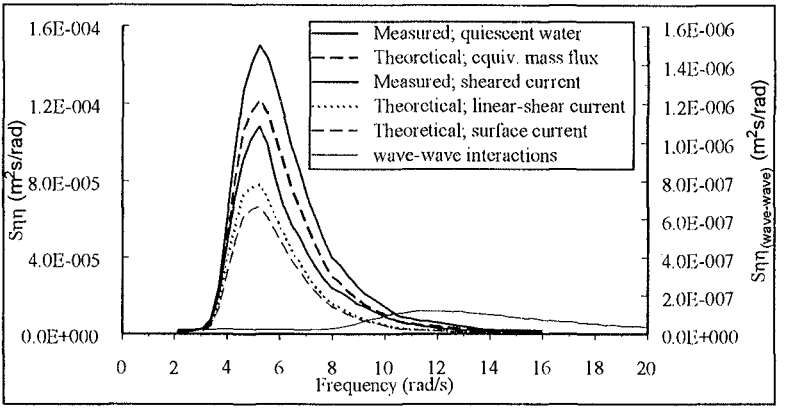

(b)

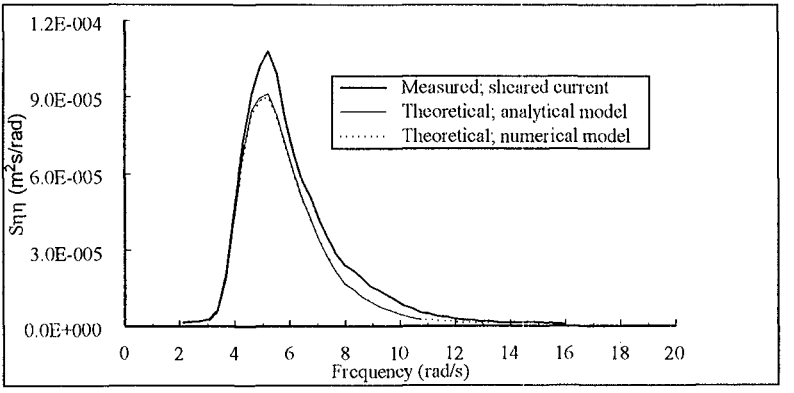

Figure 6a-6b. Changes in a nonlinear spectrum

In Figure 6b the results are (unfortunately) somewhat different from those given on figure 5b. In this case, the comparisons suggest that neither of the present methods provide a good description of the spectral changes, although they do represent a significant improvement over the solutions indicated on figure 6a. However, it is interesting to note that the apparent shortcomings are equally applicable to both the numerical calculations and the second-order analytical model. This suggests that the 'errors' do not arise as a result of higher-order nonlinear terms within the wave-current interaction. Indeed, the present results confirm that the weakly nonlinear analytical model is more widely applicable than one might expect.

The most probable explanation for the 'errors' in figure 6b lie in our treatment of the current profile. In previous studies, concerning regular waves on a vertically-sheared current, considerable effort was made to determine the current profile in the presence of the waves. Indeed, good agreement between the measured and predicted oscillatory velocities was only achieved when this profile was applied within either the analytical solution or the numerical model. In the present case this approach has not been adopted. Indeed, the results presented in figures 5 and 6 were calculated using the current profile measured in the absence of waves. The reason for this difference is clear. In a regular wave case the magnitude of the current was calculated along an empirically determined streamline. This approach allows the characteristics of the current, in particular its gradient, to be determined close to the water surface. In random waves it is simply not possible to undertake such an approach.

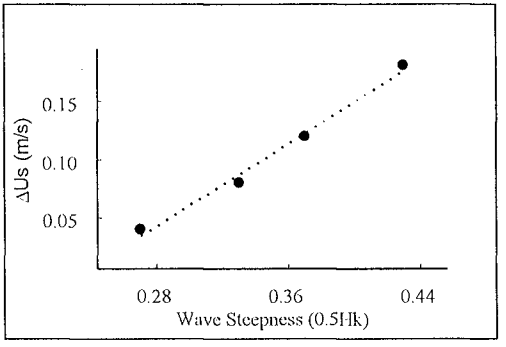

Figure 7. Changes in the surface current (regular waves)

Nevertheless, if we return to our previous regular wave data, it is clear that the extent of the current change is dependent upon the wave height, or more probably the wave steepness. For example, figure 7 considers four regular wave cases and describes the change in the magnitude of the surface current as a function of the wave steepness. Taking into account this change, it is clear that as the steepness of a random sea-state increases, the present methods will provide less reliable results. Furthermore, it is clear that if the change in a wave spectrum due to the interaction with a current is to be adequately predicted, the change in the current due to the presence of the waves must be defined. Recent work by Groeneweg and Klopman (1998) provide a possible method for investigating this effect. However, if the results of recent regular wave studies are to be believed, it would appear that in random waves the current profile will be continuously changing as it attempts to adjust to the local (or instantaneous) wave conditions. In such circumstances it may be very difficult to separate those parts of the fluid motion that relate individually to the wave and the current.

In an attempt to account for the extent of the current change, Δu, particularly that arising close to the water surface, the present study has reconsidered the current change arising in several regular wave cases, and has applied a similar change to the present

study. Having identified a 'modified' current profile, the iterative calculations were repeated and a new wave spectrum determined. The results of this procedure are presented on figure 8. This is identical to the case considered in figures 6a and 6b, and contrasts the spectrum measured in the presence of the waves with two predictions based on the analytical formulation. The first assumes the current remains unchanged; while the second is based upon our best estimate of the changed current profile. The improvement in the solution is clearly significant, and highlights the importance of the wave-induced current change. However, it should be noted that although the peak of the spectrum is in good agreement, its overall shape is no longer self-similar. This clearly raises the possibility of significant energy transfers within the spectrum due to subtle changes in the current profile.

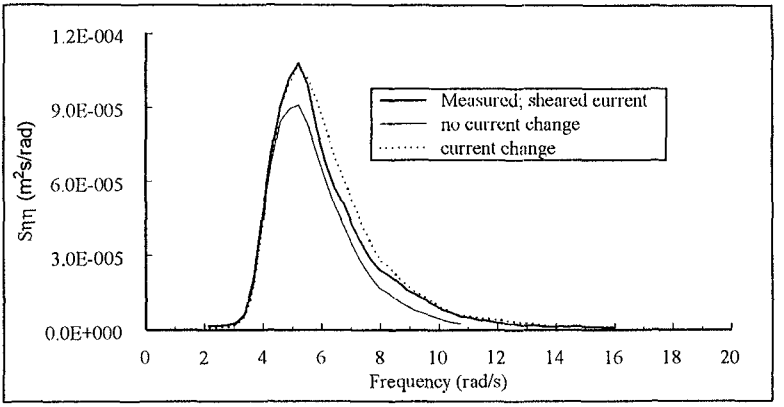

Figure 8. Spectral predictions based on a changed current

5. Concluding Remarks

The present paper has considered the modification of a random wave spectrum due to the interaction with a depth-varying current. New experimental data has been presented, and the results shown to be in reasonable agreement with a new calculation procedure based upon the conservation of total energy flux. Although this solution represents a significant improvement over existing design methods (traditionally based upon a uniform current approximation), difficulties remain concerning the description of a current profile in the presence of waves. Indeed, the present study has clearly demonstrated that in the case of a depth-varying current, the nature of the wave-current interaction involves both a current-induced change in the wave motion, and a wave-induced change in the current. Finally, the present study has also shown that a relatively simple, weakly nonlinear, analytical solution can be surprisingly effective, and provides clear guidance as to the importance of the vorticity distribution.

Acknowledgement

This work was undertaken as part of the MAST project 'The Kinematics and Dynamics of Wave-Current Interactions'. It was funded by the Commission of the European Union Directorate General for Science, Research and Development under contract No. MAST3-CT95-0011.

References

Baldock, T. E., Swan, C. and Taylor, P. H. (1996) A laboratory study of nonlinear surface waves on water. *Phil. Trans. R. Soc., Lond.* A **354**, 649-676.

Bretherton, F. P. and Garrett, G. J. R. (1968) Wavetrains in inhomogeneous moving media. *Proc. Roy. Soc.*, A **302**, 529-554.

Chaplin, J. R. (1990) The computation of nonlinear waves on a current of arbitrary non-uniform profile. OTH 90327, HMSO.

Cummins, I. and Swan, C. (1993) Nonlinear wave-current interactions. *Wave Kinematics and Environmental Forces. Society for Underwater Tech.*, Vol. **29**, pp. 35-51.

Dalrymple, R. A. (1974) Water waves on a bilinear shear current. *Proc. 14th Conf. Coastal Eng., Hamburg*, pp. 626-641.

Fenton, J. D. (1985) A fifth-order Stokes theory for steady waves. *J. waterway, Port, Coastal and Ocean Eng., ASCE*, Vol. **111**, pp. 216-234.

Groeneweg, J. and Klopman, G. (1998) Changes of the mean velocity profiles in the combined wave-current motion described in GLM formulation. Accepted for publication in *J. Fluid Mech.*

Jonsson, I. G., Brink-Kjær, O. and Thomas, G. P. (1978) Wave action and set-down for waves on a shear current. *J. Fluid Mech.*, Vol. **87**, 401-416.

Kishida, N. and Sobey, R. J. (1988) Stokes theory for waves on a linear shear current. *J. Eng. Mech., ASCE*, Vol. **114**, pp. 1317-1334.

Longuet-Higgins, M. S. and Stewart, R. W. (1960) Changes in the form of short gravity waves on long waves and tidal currents. *J. Fluid Mech.*, Vol. **8**, pp. 565-583.

Swan, C. (1992) A stream function solution for waves on a strongly sheared current. *Proc. 23rd. Int. Conf. Coastal Eng., Venice,* Vol. **1**, pp. 684-697.

Swan, C. and James, R. L. (1998) A simple analytical model for surface water waves on a depth-varying current. Submitted to *J. Geophys. Res.*

Swan, C., Cummins, I. P. and James, R. L. (1998) An experimental study of 2-D surface water waves propagating on depth-varying currents. Part 1: Regular waves. Submitted to *J. Fluid Mech.*

Thomas, G. P. (1990) Wave-current interactions: an experimental and numerical study. Part 2. Nonlinear waves. *J. Fluid Mech.* Vol. **216**, pp. 505-536.

Thomas, G. P. and Klopman, G. (1997) Wave-current interactions in the near-shore region. *In 'Gravity waves in water of finite depth', Ed. J. N. Hunt, Advances in Fluid Mechanics, Computational Mechanics Publications*, pp. 255-319.

Tsao, S. (1959) Behaviour of surface waves on a linearly varying flow. *Tr. Mosk. Fiz.-Tekh. Inst. Issled. Mekh. Prikl. Mat.*, Vol. **3**, pp. 66-84.